

## CHARACTERIZATION OF ON-WAFER DIODE NOISE SOURCES

J. Randa, D. Walker, L. Dunleavy\*, R. Billinger, and J. Rice†

Electromagnetic Fields Division  
National Institute of Standards and Technology  
Boulder, CO 80303

**Keywords:** Noise; noise measurement; noise source; on-wafer measurement; noise characterization; noise temperature.

**Abstract:** A set of wafer probeable diode noise source transfer standards are characterized using on-wafer noise temperature methods developed recently at the National Institute of Standards and Technology (NIST). This paper reviews the methods for accurate on-wafer measurements of noise temperature and details the preliminary design and construction of the transfer standards. Measurements are presented of their noise temperatures at frequencies from 8 to 12 GHz. Such transfer standards could be used in interlaboratory comparisons or as a verification tool for checking on-wafer noise calibration accuracy.

### 1. Introduction

NIST has recently developed the capability to accurately measure 1-port noise temperature on a wafer or on a substrate that can be tested using microwave wafer probes (in this paper the term “on-wafer” refers to either a substrate or a wafer) [1,2]. This capability is a stepping stone toward the development of 2-port on-wafer noise figure and/or noise-parameter measurements at NIST. The 1-port noise temperature measurement capability can also be useful in its own right, providing a means for others to confirm on-wafer noise measurement calibrations. For example, practical

calibrations for 2-port on-wafer noise measurements involve transferring the known off-wafer temperature, or equivalently excess noise ratio (ENR), of a coaxial diode noise source to an on-wafer reference plane [3]. The availability of an on-wafer noise source with known ENR's or temperatures would provide an independent verification tool for on-wafer noise measurement calibrations.

The present work lays the groundwork for one approach to on-wafer noise interlaboratory comparisons. In this approach, the noise temperatures of diode-based on-wafer noise sources would be measured at NIST and then at other laboratories interested in comparing their results. Appropriate on-wafer noise sources are not yet available. As a step towards developing such sources, this paper reports on the preliminary design, construction, and testing of on-wafer diode-based noise sources.

In the next section, we review the experimental setup and general formulation used in measuring on-wafer noise temperature. We present results of a set of related verification measurements. Section 3 is devoted to the on-wafer diode noise sources, first describing their design and then presenting the results of measurements of their noise temperatures. Finally, in Section

---

\* On leave from: Dept. of Electrical Engineering, University of South Florida, Tampa, FL.

† Present address: National Weather Service, Negaunee, MI.

U.S. Government work, not covered by U.S. copyright.

4, we summarize the results and discuss applications and future directions.

## 2. Measurement Methods and Checks

### 2.1 Measurement Configurations

Figure 1 contains a block diagram of the NIST experimental setup for the measurement of on-wafer noise temperatures, with relevant reference planes numbered. The radiometer used in the measurements also contained an isolator, so there were isolators immediately to the left and right of plane 0. The radiometer is similar in design to that used in previous tests [1,2], but is a developmental unit that has not been fully qualified for calibration services. The cryogenic and ambient standards are used to calibrate the radiometer. The radiometer is switched between the ambient standard noise source (plane 1), the cryogenic standard noise source (plane 2), and the on-wafer device (plane 7), measuring and recording the delivered power from each. A previously measured high-temperature coaxial diode noise source, or “check” standard, is connected at plane 6. Its noise temperature is also measured to confirm the proper operation of the radiometer. Reflection coefficients and S-parameters of various parts of the system, needed for computing the desired on-wafer noise temperatures [1], are measured using a vector network analyzer (VNA) in conjunction with NIST’s MultiCal<sup>®</sup> software [7].

Figure 1 also depicts the configuration used to verify the on-wafer noise temperature measurements using known off-wafer standards. This is done by connecting either a diode check standard or cryogenic standard to reference plane 10 and measuring the noise power delivered at reference plane 5 with both probes connected through an on-wafer transmission line. When the cryogenic standard is measured in this way, the check standard is used as the

nonambient standard in the calibration of the radiometer.

The configuration of Fig. 2 was used to measure the on-wafer diode sources. The bias for the on-wafer diode is supplied through probe 2 from an off-wafer current source.

### 2.2 Formulation

We first define our notation. Available powers will be denoted by a capital  $P$  and delivered powers by lowercase  $p$ . The subscript on an available power generally indicates the device, except in the case of  $P_a$ , where it indicates the ambient. The subscripts on the powers and mismatch factors will indicate the reference plane and the switch setting. The device under test (DUT) will be labeled by  $x$ . Thus  $p_{2,x}$  refers to the delivered power at plane 2 when the radiometer is switched to the DUT.

The noise temperature,  $T_x$ , of the unknown 1-port device (a diode source, for example) at on-wafer reference plane 7 of Fig. 2 is given by the radiometer equation. Assuming perfect isolators and a linear radiometer, it takes the form [1]

$$T_x = T_a + (T_S - T_a) \frac{M_{0,S} \alpha_{02} (Y_x - 1)}{M_{0,x} \alpha_{07} (Y_S - 1)} \quad (1)$$

where  $Y_x \equiv p_x / p_a$ ,  $Y_S \equiv p_S / p_a$ .  $p_x$  is the delivered noise power measured by the radiometer with the switch connected to plane 7. Similarly  $p_S$  is the delivered power measured with the switch to plane 2, and  $p_a$  is that measured with the switch to plane 1.  $T_S$  is the known temperature of the cryogenic standard, and  $T_a$  is the ambient standard temperature.  $M_{0,x}$  is the mismatch factor at plane 0 when the radiometer is switched to plane 5 in Fig. 1, and  $M_{0,S}$  is the mismatch factor at plane 0 when the radiometer is

switched to plane 2 in Fig. 1. Finally,  $\alpha_{ij}$  denotes the available-power ratio from plane  $j$  to plane  $i$ . These are defined formally by:

$$M_{0,x} = \frac{P_{0,x}}{P_{0,x}} = \frac{\text{Delivered power at 0 with switch to 5}}{\text{Available power at 0 with switch to 5}},$$

$$M_{0,s} = \frac{P_{0,s}}{P_{0,s}} = \frac{\text{Delivered power at 0 with switch to 2}}{\text{Available power at 0 with switch to 2}},$$

$$\alpha_{ij} = \frac{P_i}{P_j} = \frac{\text{Available power at } i}{\text{Available power at } j}.$$

The measurement complications associated with the on-wafer environment show up in generalized expressions for the mismatch factors and available-power ratios [1]. This is due to the more complicated form of the power equation for transmission lines with significant loss [4,5]. Equation (1) is the usual form of the radiometer equation for an isolated total-power radiometer [1, 2, 6]. In terms of traveling-wave amplitudes, complex characteristic impedance, and reflection coefficients, the expressions are unwieldy [1]. However, they can be transformed into simpler forms by the use of “pseudo-waves” [6].

Pseudo-waves are particular linear combinations of traveling waves which depend on a reference impedance of the user’s choice and on the characteristic impedance of the line. The transformation to pseudo-waves induces a corresponding transformation of reflection coefficients and S-parameters at the affected reference plane(s). If we choose a real reference impedance (typically 50  $\Omega$ ), pseudo-waves and their associated S-parameters result in the familiar, lossless-line forms for the available and delivered powers. Consequently, ratios of powers, such as mismatch factors and available-power ratios, also revert to their lossless-line forms. In the radiometer equation, the ratio of mismatch factors and available-power ratios becomes

$$\frac{M_{0,s} \alpha_{02}}{M_{0,x} \alpha_{07}} = \frac{|S_{21}^{(50)} (2 - 0)|^2}{|S_{21}^{(50)} (7 - 0)|^2} \quad (2)$$

$$* \frac{|1 - \Gamma_x^{(50)} \Gamma_{7,r}^{(50)}| (1 - |\Gamma_{2,s}^{(50)}|^2)}{|1 - \Gamma_s^{(50)} \Gamma_{2,r}^{(50)}| (1 - |\Gamma_x^{(50)}|^2)}$$

where the superscript (50) indicates that the reflection coefficient or S-parameter is referenced to a 50  $\Omega$  impedance. The various  $\Gamma$ ’s denote the reflection coefficients looking both ways from reference planes 2 and 7.

The price paid for the simplification engendered by pseudo-waves is that the reflection coefficients and S-parameters must be transformed from the usual traveling-wave values to the reference impedance chosen. In this work we used the NIST-developed package MultiCal [7], with a multiple line thru-reflect-line (TRL) calibration [8] to characterize the probes. MultiCal can determine pseudo-wave quantities, and this feature was used for all the reflection coefficients and S-parameters appearing in Eq. (2). The complex characteristic impedance,  $Z_0$ , of the on-wafer coplanar waveguide (CPW) calibration lines were determined using NIST developed methods [9] and are tabulated in Table 1.

Table 1. Measured  $Z_0$  for On-wafer Lines

Freq. (GHz)	8	9	10	11	12
Re ( $Z_0$ )	50.68	50.66	50.61	50.58	50.56
Im ( $Z_0$ )	-1.56	-1.45	-1.32	-1.22	-1.14

### 2.3 Measurement Checks

In order to check the equipment, software, and procedures, we repeated some of the tests developed and reported earlier [1,2]. The first check was a direct, off-wafer (coaxial) measurement of a commercial diode noise source whose noise temperature is well

known from past measurements. The noise temperature was measured at 8, 9, 10, 11, and 12 GHz. This off-wafer check-standard test was repeated several times during the diode measurements, using the configuration of Fig. 2. The results agreed with past measurements within 1% in almost all cases (worst case was 1.25%). Although better agreement is desired for calibration service measurements, this was considered sufficient for this exploratory research. A linearity check of the radiometer was also provided for by performing two complete sets of noise temperature measurements with first 3 dB and then 6 dB IF attenuator settings within the radiometer. All noise temperature measurements presented below are an average of the two IF settings for each measurement case. The agreement between noise temperature results for the two settings was generally within 0.5%. These tests confirmed that the radiometer, primary standards, and the relevant noise temperature software were functioning properly.

As a verification measurement, known off-wafer standards were connected to the probe station in the configuration shown in Fig. 1. By measuring and correcting for the S-parameters of the probe (probe 2) and transmission line connected between reference planes 10 and 7, we computed (using relations detailed in [1]) the predicted noise temperature at on-wafer reference plane 7. This predicted temperature was then compared to the measured on-wafer noise temperature at this reference plane determined using Eq. (1) and Eq. (2).

An extensive set of such on-wafer tests of known off-wafer standards was reported earlier [1,2], and a subset of these was repeated in the present experiment. The results shown in Fig. 3 are for a diode check standard, with an off-wafer noise temperature of about 10 000 K (or ENR of 15.2 dB), at reference plane 7 in the configuration of Fig. 1. Results are shown with the probes contacting both a thru (short

CPW line) and a line (longer CPW line) on the substrate.

The 6500 K (13.3 dB ENR) on-wafer temperature for the thru line case is consistent with the approximately 2 dB of loss associated with the probe and transmission line network between planes 10 and 7. This reasoning makes use of the fact that the difference in ENR between two reference planes separated by a lossy network is approximately equal to the loss in decibels [3]. Note that there is more loss between planes 10 and 7 when the line is used, which is consistent with the lower on-wafer temperatures observed for this case. The agreement between measured and predicted values for the on-wafer noise temperature is better than 2% in all cases, which is consistent with expanded ( $2\sigma$ ) uncertainty estimates of about 2% determined previously [1,2]. Although these tests do not check all aspects of the measurements, they nevertheless provide some confidence in the general technique and in the current set of measurements.

### 3. On-Wafer Diode Noise Sources

#### 3.1 Design

The design of the on-wafer diode noise sources used in these measurements was heavily influenced by expedience. We had developed a preliminary design for the sources when a commercial firm noted that they had already fabricated similar structures on alumina substrates and offered to provide them to us. Although these structures could not be measured in a manner completely consistent with NIST's on-wafer TRL calibration set, they saved us the trouble of fabricating on-wafer structures for this first iteration. To our knowledge these structures had never been assembled or tested. A second company provided the bare noise diodes and a circuit to supply the bias current for the diodes.

The on-wafer noise source is depicted in Fig. 4. It consists of a noise diode bonded to a section of coplanar waveguide, with an integrated attenuator between the diode and the output. Three different on-wafer sources (labeled A, B, and C) were built and tested, with three different attenuation values of nominally 10 dB (A), 15 dB (B) and 20 dB (C). The bias current for the diode was supplied from an off-wafer source (Fig. 2), through a probe contacting the pads at the left of Fig. 4. A blocking capacitor isolates the attenuator and the rf section from the DC bias. The reference plane for the noise-temperature measurements, plane 7 in Fig. 2, is at the RF port at the right in Fig. 4.

The fact that the output does not include a section of coplanar waveguide identical to half the thru line used in the on-wafer calibration kit introduces a complication not present in our earlier measurements. In the on-wafer TRL calibration used [7, 8], the probe is defined to extend to the middle of the calibration thru line. It thus includes a short (0.25 mm) section of coplanar waveguide, which is not present when the probe is set down on the pads on the right of Fig. 4. We must therefore translate the probe calibration to the probe tip to reduce the errors incurred by the lack of an appropriate access line.

This procedure neglects the effect of evanescent modes, or transition fields, in the vicinity of the probe tip. These effects could introduce errors into noise measurements; however, these concerns are ignored for the present set of exploratory measurements. Designs of future on-wafer noise sources will include a section of coplanar waveguide identical to that used in the set of on-wafer TRL calibration standards. Ideally, the TRL calibration set and noise sources will reside on the same wafer or substrate.

### 3.2 Measurement Results

Using the configuration of Fig. 2, and calculations enabled by Eqs. (1) and (2), we characterized the noise temperatures for the three on-wafer diode sources across the 8 to 12 GHz frequency range. The noise temperatures are plotted in Fig. 5, with the corresponding (available) ENR in Fig. 6. The noise temperature  $T_x$  and ENR are related by

$$\text{ENR(dB)} = 10 \log_{10} \left( \frac{T_x - T_0}{T_0} \right) \quad (3)$$

with  $T_0 = 290$  K. The noise temperature is approximately constant across the frequency range measured. The three sources have noise temperatures of about 1200 K, 3400 K, and 10 000 K, corresponding to ENRs of about 5 dB, 10 dB, and 15 dB.

The 5 dB drop in ENR observed in moving from noise source A to B and from B to C (Fig. 6) is consistent with that expected from the 5 dB successive increase in pad attenuation values for sources A (10 dB), B (15 dB), and C (20 dB). We can also infer that the ENR of the bare noise diodes used in the noise sources studied here is on the order of 25 dB.

Reflection coefficients for the three dc-biased noise sources were measured using MultiCal in conjunction with ANA measurements. The magnitudes ranged from about 0.04 to 0.12. This reflection coefficient range is much more acceptable for a noise source transfer standard as compared to the bare (nonpadded) noise diodes measured in the prior work [1], which had a reflection coefficient magnitude of around 0.8.

## 4. Summary

We have assembled on-wafer diode noise sources and tested them over the 8-12 GHz frequency range. Although the radiometer

system used for the measurements is still under development, the many checks performed in conjunction with the principal measurements yielded reassuring results. The sources have noise temperatures ranging from about 1000 K to about 10 000 K, corresponding to excess noise ratios from about 5 dB to about 15 dB, and are only weakly dependent on frequency. Their reflection coefficients in the biased state range from about 0.04 to about 0.11.

The noise sources represent a significant step in the development of practical artifacts, which could be used to test or compare on-wafer noise measurements at different laboratories or to confirm the repeatability of measurements at a given laboratory. We plan to refine the design and to build and test a second generation of such sources.

#### Acknowledgments

We are grateful to Eric Strid and Leonard Hayden of Cascade Microtech for providing the basic on-wafer structures, and to Kevin Kerwin of Hewlett Packard for providing the biasing circuit and the noise diodes. This work was funded in part by the NIST/Industrial MMIC Consortium.

#### References

- [1] J. Randa, "Noise temperature measurements on wafer," Natl. Inst. Stand. Technol. Tech. Note 1390, March 1997.
- [2] J. Randa, R.L. Billinger, and J.L. Rice, "On-wafer measurements of noise temperature," submitted to IEEE Trans. Instrum. Meas., 1997.
- [3] L. Dunleavy, "A Ka-band on-wafer s-parameter and noise figure measurement system,," 34<sup>th</sup> ARFTG Conference Digest; Ft. Lauderdale, FL; Dec. 1989. 127-137.
- [4] N. Marcuvitz, *Waveguide Handbook*; McGraw-Hill, NY, 1951, and Peter Peregrinus, London, 1986; Ch. 1.
- [5] R. Marks and D. Williams, "A general waveguide circuit theory," J. Res. Natl. Inst. Stand. Technol., vol. 97, pp. 533-562, Sept./Oct. 1992.
- [6] W.C. Daywitt, "Radiometer equation and analysis of systematic errors for the NIST automated radiometers," Natl. Inst. Stand. Technol. Tech. Note 1327, March 1989.
- [7] R. Marks and D. Williams, NIST/Industrial MMIC Consortium Software Manuals, Feb. 1992.
- [8] R. Marks, "A multilane method of network analyzer calibration," IEEE Trans. Microwave Theory Tech. Vol. MTT-39, pp. 1205-1215, July 1991.
- [9] R. Marks, D. Williams, "Characteristic impedance determination using propagation constant measurement," IEEE Microwave & Guided Wave Lett. 1(6): 141-143; June 1991.

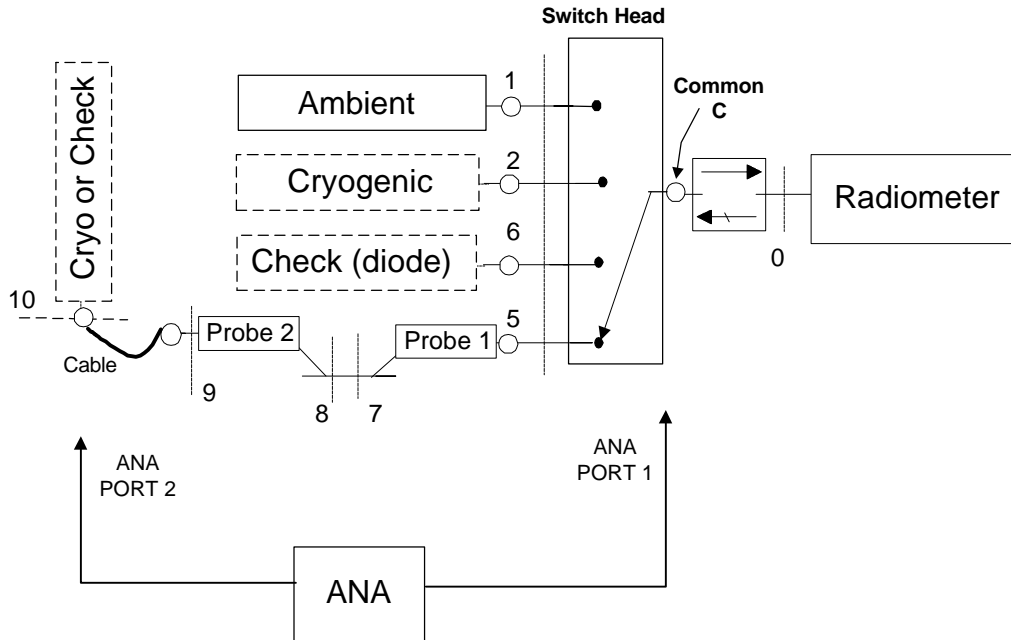


Figure 1. Configuration used for ANA characterization of the test system and for measurement of off-wafer cryogenic and diode “check” standards through probe networks.

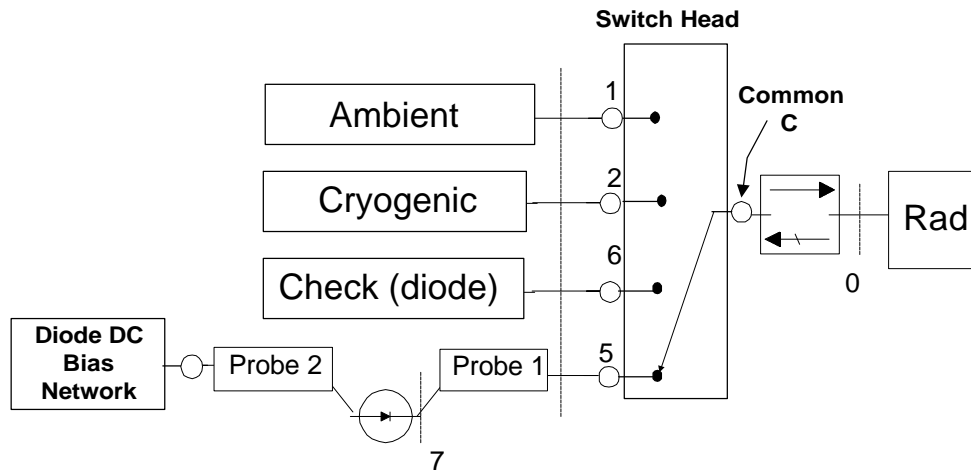


Figure 2. Configuration for characterization of on-wafer diode noise sources. Bias is applied through probe.

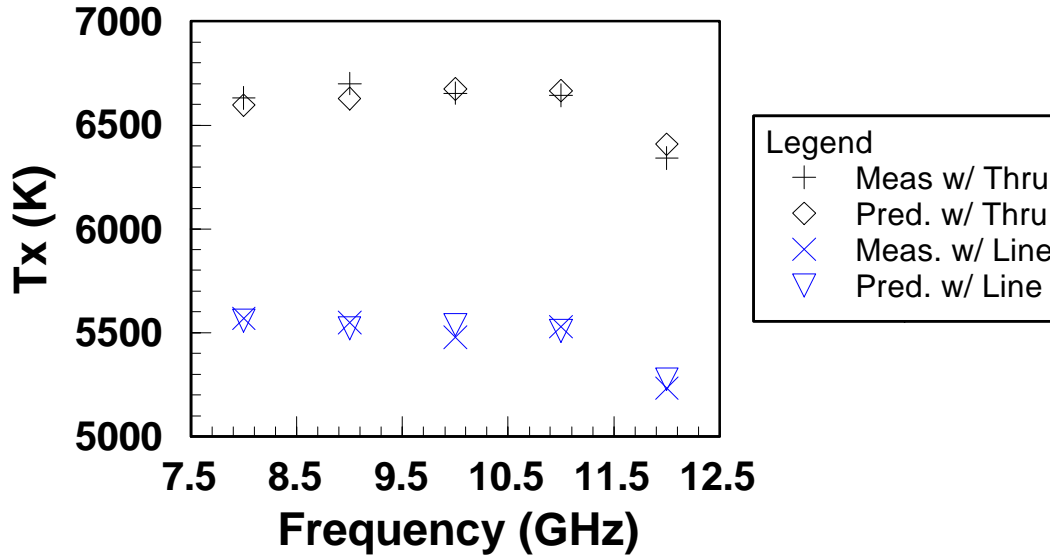


Figure 3. Comparison of measured and predicted on-wafer temperature (at plane 7 of Fig. 1) presented by a coaxial diode noise source connected to probe 2. Measurements were made with both a short (thru) and long (line) CPW line connected between the probes.

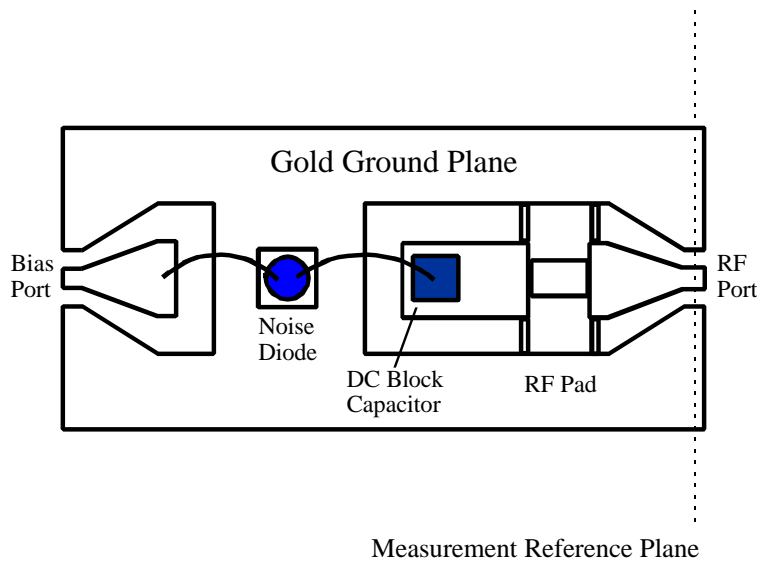


Figure 4. Layout for wafer probeable diode noise source layout used in this work. Diodes with three different attenuator (pad) values were used, labeled Diode A, Diode B, and Diode C.

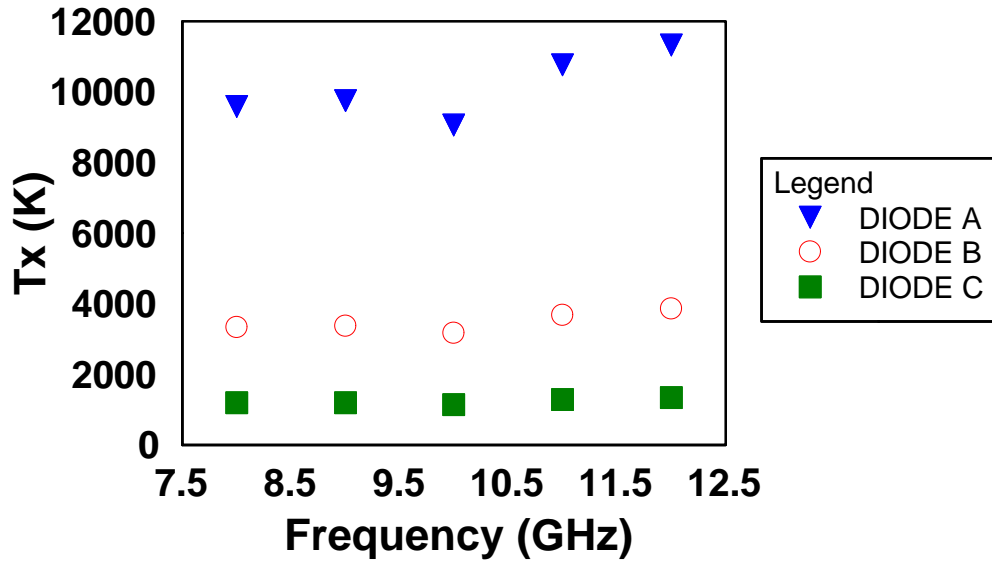


Figure 5. Measured on-wafer temperature of wafer probeable diode noise sources with integral pads of three different attenuation values.

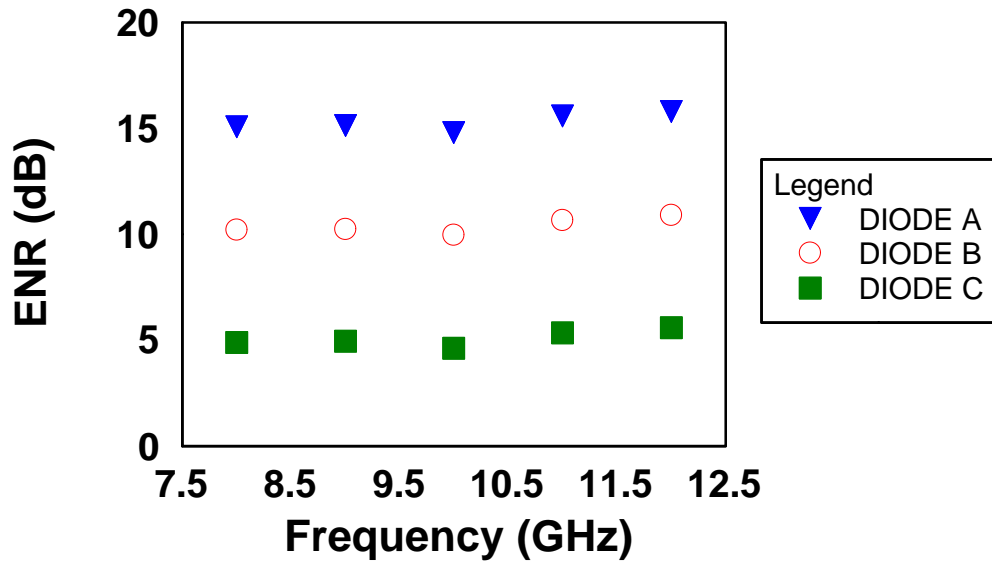


Figure 6. Excess Noise Ratio (ENR) corresponding to measured on-wafer temperature of the three wafer-probeable diode noise sources.